PHYSICAL PROPERTIES OF LYMAN ALPHA FOREST CLOUDS

12.1 Absorption Line Formation

In this lecture we are going to look at some of the steps involved in the interpretation of the Lyα absorption spectra in terms of the physical properties of the structures that produce them. As can be seen from Figure 12.1, Lyα absorption lines come in a variety of shapes and strength. In order to understand the reasons for this diversity, we have to review how absorption lines are formed.

Consider a plane parallel slab of gas of thickness L along a coordinate x, so that x varies from 0 to L. The intensity of light of wavelength λ incident upon the slab at $x = 0$ is $I_{\lambda,0}$. The incremental extinction of the intensity of light over an infinitesimal distance from x to $x + dx$ is

$$dI_\lambda = -a_\lambda n I_\lambda dx \tag{12.1}$$

where a_λ (which has the units of a cross-section, that is cm^2) is the line absorption coefficient describing the absorption of photons by bound-bound atomic transitions, and n is the volume density of absorbing gas atoms (cm^{-3}). Following the absorption to a higher energy level, the electron falls back to its original state (possibly via intermediate states) re-emitting

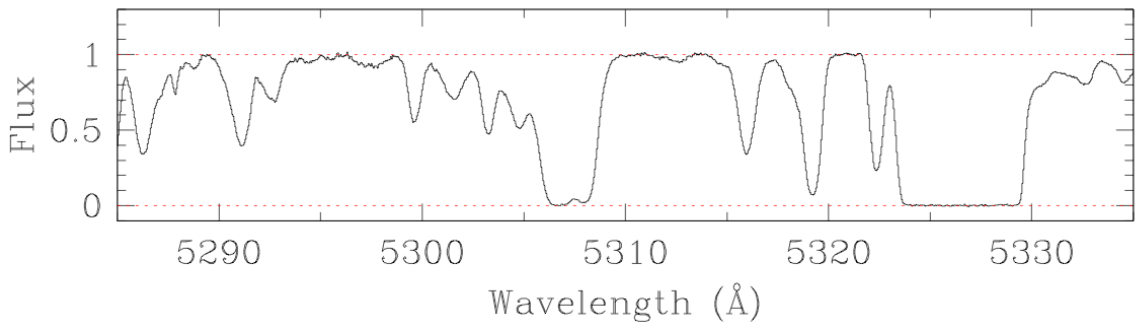

Figure 12.1: Typical Lyα forest lines at redshift $z_{\rm abs} \sim 3.5$

a photon (or photons). However, since such photons are re-emitted in a random direction, they are effectively scattered out of the observed line of sight to the background source.

The optical depth at wavelength λ

$$\tau_\lambda = \int_0^L a_\lambda n \, dx \tag{12.2}$$

is the integrated absorption of I_λ emerging from the slab at L, so that we can re-write eq. 12.1 as

$$dI_\lambda = -I_\lambda d\tau_\lambda \tag{12.3}$$

which has the solution

$$I_\lambda = I_{\lambda,0} \, e^{-\tau_\lambda} \tag{12.4}$$

or

$$\frac{I_\lambda}{I_{\lambda,0}} = e^{-\tau_\lambda} \tag{12.5}$$

and

$$\tau_\lambda = N \cdot a_\lambda \tag{12.6}$$

where N is the *column density* of absorbing atoms or ions (number of absorbers per unit area, with units cm^{-2}).

The quantity $I_\lambda / I_{\lambda,0}$ is the *Residual Intensity* and this is what is plotted on the y-axis of Figure 12.1. Thus, if we can measure $I_\lambda / I_{\lambda,0}$ from a spectrum of the Lyα forest, we can deduce the column density of hydrogen atoms absorbing at a particular wavelength, $N(\lambda)$ [knowing the atomic parameter a that describes the probability of a given transition taking place (see later)].

If we are interested in a particular wavelength (or velocity) interval, we can just add up the values of N within that interval to deduce the total column density within a given absorbing 'cloud'. For the Lyman α line:

$$N(v) = 7.45 \times 10^{11} \cdot \tau(v) \;\; \text{cm}^{-2} \left(\text{km s}^{-1}\right)^{-1} \tag{12.7}$$

and

$$N(\text{H I})_{\text{tot}} = \sum_1^n N(v) \cdot d(v) \tag{12.8}$$

where the summation is over the n velocity intervals, each of width $d(v)$ (km s^{-1}), spanned by the absorption line.

12.2 Line Equivalent Width

The above treatment is valid provided we can measure $I_\lambda/I_{\lambda,0}$ directly. This is only possible if the instrument used to record the QSO spectrum has sufficient resolution to maintain the intrinsic shapes of the absorption lines. While this is now generally the case when it comes to spectroscopy of the Lyα forest, the situation was different in the past, when astronomical instrumentation and telescopes were less advanced. In cases where an imperfect instrument smears out the QSO spectrum so that the intrinsic line profiles are no longer measurable, we are forced to resort to the concept of *Equivalent Width*. Furthermore, even in the best spectra, such as the data shown in Figure 12.1, it can be appreciated that when $\tau_\lambda \gg 1$, $I_\lambda/I_{\lambda,0} \simeq 0$, and we can no longer recover N in the black cores of strong lines. Nevertheless, the concept of equivalent width may still be useful in some circumstances.

The equivalent width W_λ of an absorption line is defined as the width, in wavelength units, of a rectangular strip of spectrum having the same area as the absorption line. That is, it is the width that the line would have, for

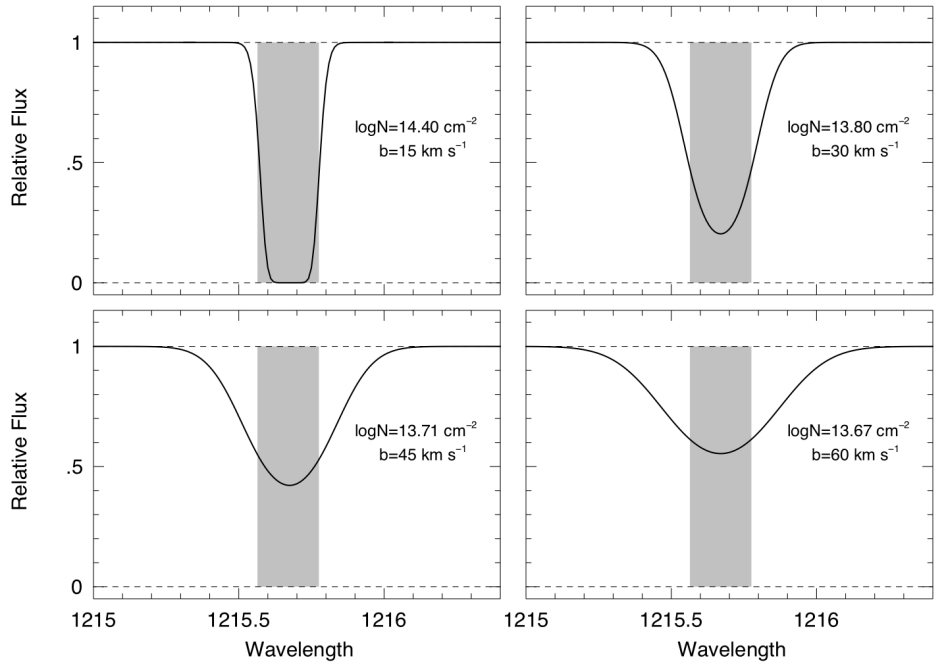

Figure 12.2: Four Lyα lines with the same equivalent width (shaded grey area) but different widths (and column densities). The Doppler parameter b describes the motion of the absorbing atoms. (Figure courtesy of Chris Churchill).

the same energy taken out, if the intensity of the line were zero everywhere. With this definition:

$$W_\lambda = \int \frac{I_{\lambda,0} - I_\lambda}{I_{\lambda,0}}\, d\lambda \;=\; \int \left(1 - e^{-\tau_\lambda}\right)\, d\lambda \tag{12.9}$$

The value of the equivalent width is that it is *invariant* to convolution of the intrinsic QSO spectrum with the resolution of the instrument used to record it.

Returning to eq. 12.6, the line absorption coefficient at wavelength λ can be written as:

$$a_\lambda = a_0 \cdot \Phi_\lambda \tag{12.10}$$

where a_0 includes the atomic parameters of the transition

$$a_0 = \frac{\lambda^4}{8\pi c}\, \frac{g_k}{g_1}\, a_{k1} \tag{12.11}$$

where g_k and g_1 are the statistical weights of the excited and ground energy levels, a_{k1} is the transition probability and the other symbols have their usual meaning.

Φ_λ is the broadening function, defined so that if an absorption does take place in the line, $\Phi_\lambda d\lambda$ is the probability that the wavelength of the absorbed photon lies between λ and $\lambda + d\lambda$. The value of Φ_λ is large near λ_0 (the line centre) and falls off at longer and shorter wavelengths.

For atoms in intergalactic space, there are two main contributions to Φ_λ. One is 'natural broadening', ϕ_λ, resulting from the finite width of the energy level to which the absorption takes place, and the other is Doppler broadening, $\Psi(v)$, due to the velocities of the absorbing atoms. In turn, Doppler broadening has two contributions, one microscopic related to the temperature of the gas, and the other macroscopic due to large-scale motions (contraction, expansion, turbulence of the absorbing region).

The full expression for the line optical depth at wavelength λ is given by:

$$\tau_\lambda = N\, a_0\, \phi_\lambda \bigotimes \Psi(v) \tag{12.12}$$

where $\bigotimes$ is the convolution of the natural broadening and Doppler broadening functions; this expression for τ_λ is often referred to as the Voigt function.

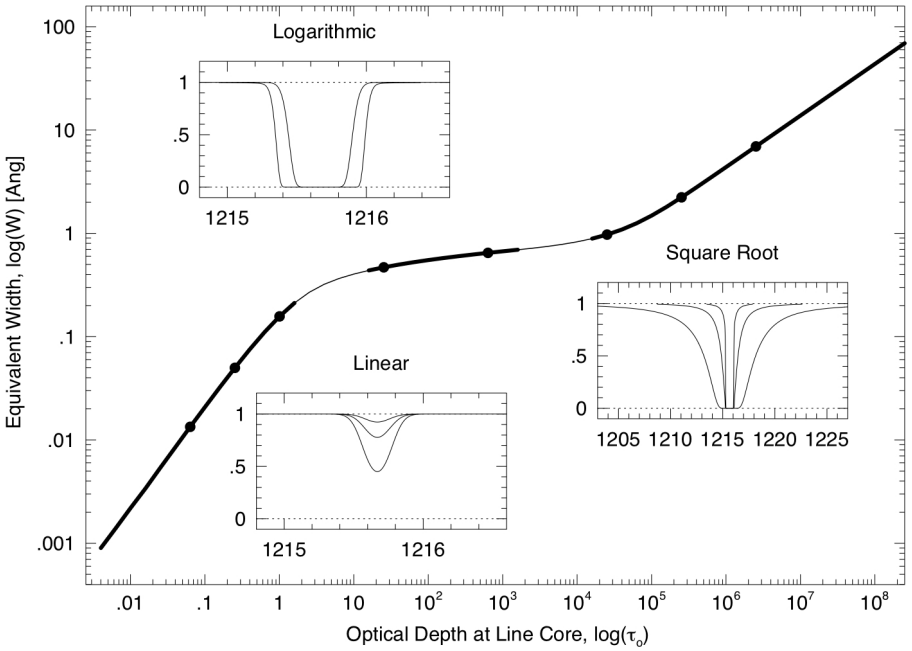

Figure 12.3: Example of a curve of growth for a Lyα line of H^0 with $b = 30\,\mathrm{km\ s^{-1}}$. The three regimes discussed in the text, the linear, flat, and damping part of the COG are shown by thicker curves. Corresponding line absorption profiles are shown for each regime and their locations on the COG are marked with filled dots. The wavelength (x-axis) scale in the panel for lines on the damping part of the COG has been expanded relative to the other two panels to illustrate the large extent of damping wings. (Figure courtesy of Chris Churchill).

Integration of 12.9 then gives the relationship between the equivalent width W_λ of an absorption line and the column density N of absorbing atoms. This relationship, which is illustrated in Fig. 12.3, is known as the Curve of Growth, because it describes how W_λ grows with increasing N.

We recognise three distinct portions of the Curve of Growth, illustrated in Fig. 12.3: 1. **The linear part**, where $\tau_0 < 1$ and $W_\lambda \propto N$. The absorption line is optically thin and W_λ is a sensitive measure of N, irrespectively of the value of the Doppler parameter b ($b = \sqrt{2}\sigma$, where σ is the one-dimensional velocity dispersion of the absorbing atoms along the line-of-sight).

2. **The flat, or logarithmic, part**, where $10 \lesssim \tau_0 \lesssim 10^3$ and $W_\lambda \propto b\sqrt{\ln(N/b)}$. The absorption line is optically thick and W_λ is *not* a good measure of N, but is sensitive to the Doppler parameter b.

3. **The damping, or square root, part**, where $\tau_0 \gtrsim 10^4$ and $W_\lambda \propto \sqrt{N}$. In this regime, the optical depth in the damping wings provides an accurate estimate of N.

For an optically thin (i.e. on the linear part of the curve-of-growth) Lyα line:

$$N(\mathrm{H\,I}) = 1.84 \times 10^{14} \cdot \mathrm{W}_\lambda \ \ \mathrm{cm}^{-2} \tag{12.13}$$

(with W_λ measured in Å). Therefore a Lyα absorption line with an equivalent width (in the rest frame, of course!) $W_\lambda = 100\,\mathrm{m\AA}$ corresponds to neutral hydrogen column density $N(\mathrm{H\,I}) \simeq 2 \times 10^{13}\,\mathrm{cm}^{-2}$.

On the other hand, for a damped Lyα line:

$$N(\mathrm{H\,I}) = 1.88 \times 10^{18} \cdot W_\lambda^2 \ \ \mathrm{cm}^{-2} \tag{12.14}$$

(with W_λ measured in Å), so that $N(\mathrm{H\ I}) = 2 \times 10^{20}$ cm^{-2} corresponds to $W_\lambda \simeq 10\,\mathrm{\AA}$. (In practice, however, it is more common to use the profile of the damping wings to deduce $N(\mathrm{H\,I})$, because it becomes impractical to measure the equivalent width of an absorption line with extended damping wings.)

Using the methodology outlined above, it is possible to analyse the entire Lyα forest and deduce the column density of neutral hydrogen, $N(\mathrm{H\,I})$, of individual 'clouds' (although it is somewhat arbitrary what you call a cloud). In the next section, we are going to relate $N(\mathrm{H\,I})$ to other physical properties of intergalactic Lyα clouds.

12.3 Physical Properties of Intergalactic Lyα Clouds

We are now going to consider the scaling of $N(\mathrm{H\,I})$ with some properties that may be of interest in interpreting the nature of Lyα clouds. Although the relations given below can be deduced analytically, their derivation is beyond the scope of this course. Interested readers can refer to Schaye 2001, ApJ, 559, 507 for a complete treatment. The scalings are largely confirmed by the results of cosmological N-body simulations such as those described in the previous lecture.

12.3.1 Density of Lyα Clouds

The first scaling relates the observable $N_{\mathrm{H\,I}}$ to n_{H}, the total *volume* density of the gas, neutral and ionised:

$$N_{\rm H\,I} \simeq 2.3 \times 10^{13}\,{\rm cm}^{-2}\,T_4^{-0.26}\,\Gamma_{12}^{-1}\,\left(\frac{n_{\rm H}}{10^{-5}\,{\rm cm}^{-3}}\right)^{3/2}\left(\frac{f_{\rm g}}{0.16}\right)^{1/2} \qquad (12.15)$$

Here, T_4 is the temperature in units of $10^4\,{\rm K}$, Γ_{12} is the photoionization rate for the process ${\rm H}^0 + h\nu \Rightarrow {\rm H}^+ + {\rm e}^-$ in units of $10^{-12}\,{\rm s}^{-1}$, and $f_{\rm g}$ is the fraction of the mass in gas. In cold, collapsed clumps $f_{\rm g} \approx 1$, but on the larger scales of interest here, $f_g \simeq \Omega_{\rm b}/\Omega_{\rm m} = 0.16$.

Because the gas responsible for the low-column density Lyα forest is still expanding, it is of interest to express $n_{\rm H}$ as a density contrast over the average density of the Universe at redshift z:

$$\delta \equiv \frac{\rho - \langle\rho\rangle}{\langle\rho\rangle} \equiv \frac{n_{\rm H} - \langle n_{\rm H}\rangle}{\langle n_{\rm H}\rangle}$$

where

$$n_{\rm H} = (1+z)^3\,(1-Y)\,(1+\delta)\,\frac{3\Omega_{\rm b,0}H_0^2}{8\pi G m_{\rm H}} \qquad (12.16)$$

(Y is the baryonic mass fraction in He: $Y_{\rm p} = 0.24$) and

$$\langle n_{\rm H}\rangle \simeq 1.1 \times 10^{-5}\,{\rm cm}^{-3}\,\left(\frac{1+z}{4}\right)^3\,\frac{\Omega_{\rm b,0}h^2}{0.02} \qquad (12.17)$$

leading to:

$$N_{\rm H\,I} \simeq 2.7{\times}10^{13}\,{\rm cm}^{-2}\,(1{+}\delta)^{3/2}\,T_4^{-0.26}\,\Gamma_{12}^{-1}\,\left(\frac{1+z}{4}\right)^{9/2}\left(\frac{\Omega_{\rm b,0}h^2}{0.02}\right)^{3/2}\left(\frac{f_{\rm g}}{0.16}\right)^{1/2} \qquad (12.18)$$

From the above, we deduce that **the low-column density Lyα forest traces gas of low overdensity**. Note the following:

• Overdensities $\delta > 100$ (virialised mini-halos) correspond to high column density systems (the metal-line systems) with $N_{\rm H\,I} > 1 \times 10^{16}\,{\rm cm}^{-2}$.

• The presence of dark matter does not have a dramatic effect on the correspondence between $N_{\rm H\,I}$ and δ. If $f_{\rm g} = 1$, the density contrast corresponding to a given $N_{\rm H\,I}$ is only a factor of two smaller.

• The steep redshift dependence is offset to some extent by the evolution of the ionising background reflected by Γ_{12}, which drops by two orders of

magnitude from $z = 3$ to $z = 0$. Thus, the value of $N_{\rm H\,I}$ corresponding to a fixed δ is only ~ 5 times lower at $z = 0$ than at $z = 3$. That is, the local Lyα forest is not fundamentally different from that at high redshift.

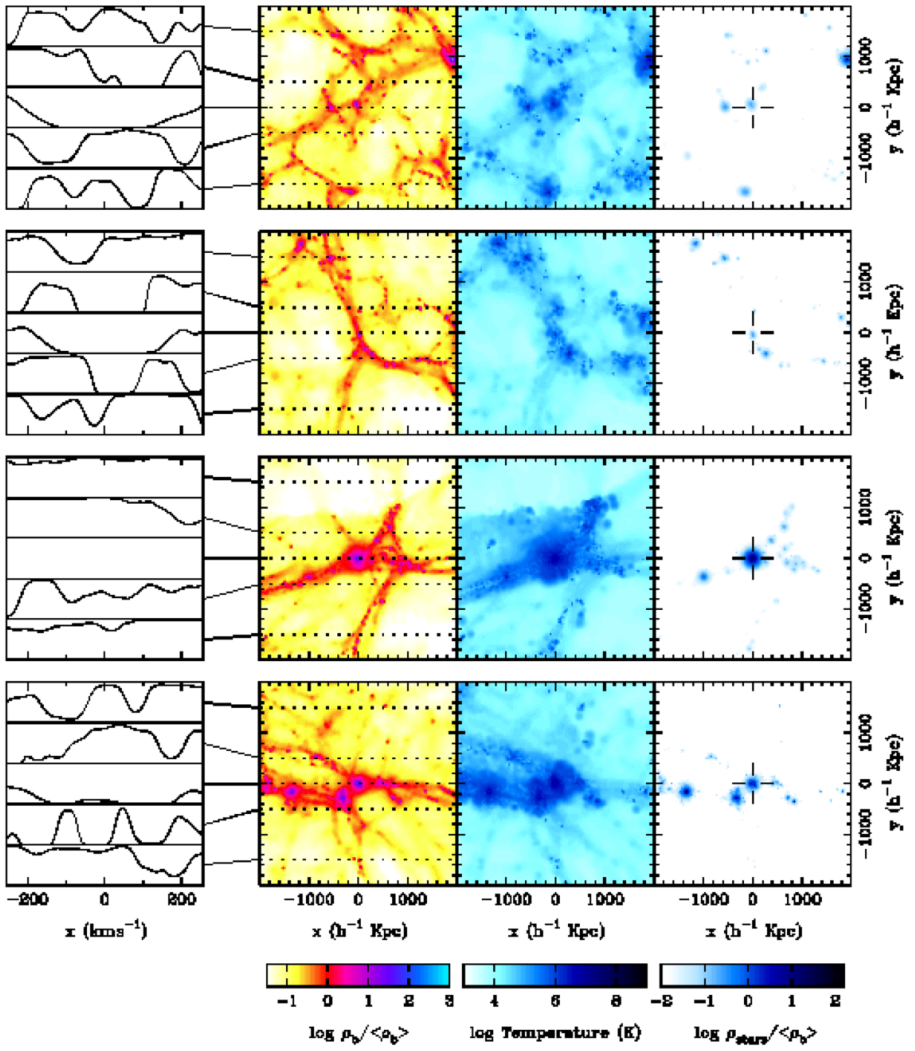

Figure 12.4: Results from a hydrodynamic computer simulation of galaxy formation, showing structure in the space around galaxies at redshift $z = 3$. Each row is for a different galaxy; the top two rows are for dwarf galaxies, and the bottom two are large, with masses more like the Milky Way. The different panels in each row show the density field (the yellowish panel), the temperature of the gas (middle panel), and the density of stars. The galaxy in each case is in the middle of the picture, and is small compared to the size of the plot. Also visible in the plots is the intergalactic gas that has yet to condense and form into stars (and is therefore not directly viewable observationally). In the simulation plot, it can be seen as a 'web' of filaments surrounding the galaxies. This gas can be detected by looking at absorption in the spectra of background quasars. The leftmost panel shows what absorption spectra would look like passing close to the galaxies. We can think of these spectra as one-dimensional maps of the gas in intergalactic space. (Simulations by Croft, Hernquist, Springel, et al.)

12.3.2 Sizes of Lyα Clouds

The second relation gives us the radial size of Lyα clouds as a function of neutral hydrogen column density:

$$L \simeq 1.0 \times 10^2 \,\mathrm{kpc} \left(\frac{N_{\mathrm{H\,I}}}{10^{14}\,\mathrm{cm}^{-2}} \right)^{-1/3} T_4^{0.41}\, \Gamma_{12}^{-1/3} \left(\frac{f_{\mathrm{g}}}{0.16} \right)^{2/3} \tag{12.19}$$

Thus, **Lyα absorbers are large structures.** 100 kpc is ~ 3 times the diameter of the Milky Way disk, and twice the distance from the Milky Way to its nearest satellite, the Large Magellanic Cloud. Note that:

• There is only a weak dependence on the temperature, the intensity of the ionising background, and the neutral H column density; even clouds with $N_{\mathrm{H\,I}} \sim 1 \times 10^{17}\,\mathrm{cm}^{-2}$ have a characteristic size $L \sim 10$ kpc.

• The physical size of an absorber at a fixed $N_{\mathrm{H\,I}}$ does not depend explicitly on redshift. The main time dependence is via Γ which, as we have seen, decreases by approximately two orders of magnitude from $z = 3$ to the present. The physical sizes of the absorbers are thus a factor of ~ 5 greater at $z = 0$ than those of $z = 3$ absorbers of the same $N_{\mathrm{H\,I}}$. However, the comoving sizes are comparable.

12.3.3 Widths of Lyα Lines

For Lyα clouds which have not decoupled from the Hubble expansion, the differential Hubble flow across the absorber broadens the absorption line leading to a Hubble width:

$$b_{\mathrm{Hubble}} \sim H(z) \cdot L/2 \text{ km s}^{-1} \tag{12.20}$$

where $H(z)$ is the Hubble parameter which, as we know (Lecture 5) is given by:

$$\frac{H(z)}{H(z=0)} = \left[\Omega_{\mathrm{m},0} \cdot (1+z)^3 + \Omega_{\mathrm{k},0} \cdot (1+z)^2 + \Omega_{\Lambda,0} \right]^{1/2} \tag{12.21}$$

i.e. $H(z=3) = 312\,\mathrm{km\ s^{-1}\ Mpc^{-1}}$ for the standard values $\Omega_{\mathrm{m},0} = 0.3$, $\Omega_{\Lambda,0} = 0.7$, $\Omega_{\mathrm{k},0} = 0.0$ and $H_0 = 70\,\mathrm{km\ s^{-1}\ Mpc^{-1}}$. On the other hand,

thermal broadening results in a b value:

$$b_{\rm T} \equiv \left(\frac{2kT}{m_{\rm H}}\right)^{1/2} = 12.8\, T_4^{1/2}\ {\rm km\ s^{-1}} \tag{12.22}$$

Thus, for clouds with column densities $N_{\rm H\,I} \simeq 1 \times 10^{14}\,{\rm cm^{-2}}$ and radial size $L \simeq 100\,{\rm kpc}$ (eq. 12.19), $b_{\rm Hubble} \approx b_{\rm T}$. Note the following:

• The Hubble width and the thermal broadening width have a similar temperature dependence: $b_{\rm H} \propto T^{0.41}$ while $b_{\rm T} \propto T^{0.5}$

• In reality, the absorbers hardly ever expand freely, but respond to the gravitational attraction of nearby structures. That is, peculiar velocity gradients will change the redshift space sizes of the absorbers.

However, peculiar velocity gradients cannot decrease the line width below $b_{\rm T}$. Thus, the minimum $b_{{\rm Ly}\alpha}$ as a function of $N_{\rm H\,I}$ can be used to measure T as a function of $n_{\rm H}$ (the equation of state).

12.3.4 Masses of Lyα Clouds

The final scaling gives the *mass* of a Lyα cloud of a given column density, under the assumption of spherical symmetry:

$$M_{\rm g} \simeq 8.8 \times 10^8 M_\odot \left(\frac{N_{\rm H\,I}}{10^{14}\,{\rm cm^{-2}}}\right)^{-1/3} T_4^{1.41}\, \Gamma_{12}^{-1/3} \left(\frac{f_{\rm g}}{0.16}\right)^{5/3} \tag{12.23}$$

Note the following:

• $M \sim 10^9 M_\odot$ is the baryonic mass of a dwarf galaxy, such as the Small Magellanic Cloud, and only $\sim 1/100$ of the baryonic mass of the Milky Way.

• The total mass is a factor $1/f_{\rm g}$ higher, when we include the dark matter.

• The mass scales *inversely* with $N_{\rm H\,I}$. This is because $n_{\rm H} \propto (N_{\rm H\,I})^{2/3}$ (eq. 12.15), while $L \propto (N_{\rm H\,I})^{-1/3}$ (eq. 12.19), and $M_{\rm g} \propto n_{\rm H}\, L^3$. Therefore,

The mass is in the lower neutral hydrogen column density absorbers.